Letter

Uncertainties on the $\overset{(-)}{\nu}_e/\overset{(-)}{\nu}_\mu$ and $\nu_e/\bar{\nu}_e$ cross-section ratio from the modeling of nuclear effects at 0.2 to 1.2 GeV neutrino energies and their impact on neutrino oscillation experiments

T. Dieminger,[1,*] S. Dolan,[2,†] D. Sgalaberna,[1,‡] A. Nikolakopoulos,[3] T. Dealtry,[4] S. Bolognesi,[5] L. Pickering,[6] and A. Rubbia[1]

[1]*ETH Zurich, Institute for Particle physics and Astrophysics, CH-8093 Zurich, Switzerland*
[2]*European Organization for Nuclear Research (CERN), 1211 Geneva 23, Switzerland*
[3]*Theoretical Physics Department, Fermilab, Batavia, Illinois 60510, USA*
[4]*Lancaster University, Physics Department, Lancaster LA1 4YB, United Kingdom*
[5]*IRFU, CEA, Université Paris-Saclay, F-91191 Gif-sur-Yvette, France*
[6]*Royal Holloway University of London, Department of Physics, Egham, Surrey TW20 0EX, United Kingdom*

(Received 5 April 2023; accepted 23 June 2023; published 14 August 2023)

The potential for mismodeling of ν_μ/ν_e, $\bar{\nu}_\mu/\bar{\nu}_e$, and $\nu_e/\bar{\nu}_e$ cross-section ratios due to nuclear effects is quantified by considering model spread within the full kinematic phase space for charged-current quasielastic interactions. Its impact is then propagated to simulated experimental configurations based on the Hyper-K and ESSνSB experiments. Although significant discrepancies between theoretical models is confirmed, it is found that these largely lie in regions of phase space that contribute only a very small portion of the flux-integrated cross sections. Overall, a systematic uncertainty on the oscillated flux-averaged $\nu_e/\bar{\nu}_e$ cross-section ratio is found to be ∼2 and ∼4% for Hyper-K and ESSνSB, respectively.

DOI: 10.1103/PhysRevD.108.L031301

Currently running accelerator-based long-baseline (LB) neutrino experiments, T2K [1,2] and NOvA [3,4], are placing increasingly tight constraints on neutrino oscillation parameters. LB experiments infer both (anti)electron neutrino appearance and (anti)muon neutrino disappearance in an (anti)muon neutrino beam using a "far" detector (FD), placed a few hundred kilometers away from the neutrino production point. LB measurements are sensitive to the neutrino oscillation parameters: θ_{23} (including the octant), the complex phase δ_{CP}, responsible for the violation of the leptonic charge-parity (CP) symmetry, and the neutrino mass-squared splittings, Δm^2_{32}, including the neutrino mass ordering (MO), i.e., whether $\Delta m^2_{32} > 0$ (normal) or $\Delta m^2_{32} < 0$ (inverted). Although the latest LB measurements remain statistically limited, their sensitivity is continuing to improve as larger samples of data are collected in higher-intensity beams [5]. The upcoming Hyper-K [6] and DUNE [7] experiments will identify the correct neutrino MO and measure δ_{CP} with a resolution better than 20°. Another experiment, ESSνSB, has proposed to further improve the resolution below 8° [8]. With an order of magnitude of more data, compared to current Experiments, future Experiments are likely to be dominated by systematic uncertainties due to the possible mismodeling of the neutrino-nucleus interaction cross sections [9]. Since the predominant sensitivity to δ_{CP}, the MO, and the octant stems from an analysis of (anti)electron neutrino appearance event rates at the FD, the uncertainty on the differences between the (anti)muon neutrino cross sections, which can be constrained at a near detector, and the FD-relevant (anti)electron neutrino cross sections, is especially important. Uncertainties on the $\nu_e/\bar{\nu}_e$ cross-section ratio are projected to be dominant uncertainty for future δ_{CP} measurements [10,11].

For interactions where the range of kinematically allowed energy- and momentum transfers is comparable to lepton mass differences, the ratio of charged-current cross sections for different flavors of neutrinos can be very sensitive to subtle nuclear effects [12–15] or radiative corrections [16]. The latter have currently been assigned a ∼2% systematic uncertainty on the $\nu_e/\bar{\nu}_e$ cross-section ratio at energies around 1 GeV [17], but recent calculations offer prospects for significant reduction [18,19].

In this article the impact of nuclear effects on the cross-section ratios (ν_μ/ν_e, $\bar{\nu}_\mu/\bar{\nu}_e$, and $\nu_e/\bar{\nu}_e$) of charged-current quasielastic (CCQE) interactions are studied. CCQE

*tilld@ethz.ch
†Stephen.Joseph.Dolan@cern.ch
‡davide.sgalaberna@cern.ch

interactions on oxygen nuclei (the dominant interaction and target for the T2K, Hyper-K, and ESSνSB experiments) are investigated across a variety of state-of-the-art and widely used models. Differences in the ratios between oxygen and carbon nuclei are also considered. A systematic uncertainty is derived to cover the observed model spread for the Hyper-K (which is also applicable to T2K) and ESSνSB experiments in the form of two correlated uncertainties on the ν_μ/ν_e and $\bar{\nu}_\mu/\bar{\nu}_e$ cross-section ratios, which together imply an uncertainty on the $\nu_e/\bar{\nu}_e$ ratio.

CCQE neutrino interactions are generated with a flat neutrino flux between 0 and 2 GeV on an oxygen target using the NEUT interaction event generator [20], using either a local Fermi gas (LFG) model (with random-phase approximation corrections) based on [21,22], or a model that uses the plane-wave impulse approximation using the Benhar spectral function (SF), based on [23]. Note that the axial mass parameter M_A^{QE} is set at NEUT's default values of 1.21 GeV for SF and 1.05 GeV for LFG, although an alternative version of SF using 1.03 GeV is also considered. Another alternative version of SF is considered in which Pauli blocking is disabled. NUISANCE [24] is used to process the simulations and to scale generated events to cross sections. The impact of statistical uncertainties was verified to be small [25].

The NEUT cross-section predictions are compared among each other and to inclusive cross-section calculations using SuSAv2 [26] or a Hartree-Fock (HF) model with and without continuum random-phase approximation (CRPA) corrections [27,28], produced using the hadron tensor tables prepared for their implementations within the GENIE event generator [29–31]. In the HF-CRPA case, the distortion of the outgoing nucleon wave function [i.e., Final State Interactions (FSI)] can be disabled so the outgoing nucleon is considered a plane wave (PW). In contrast to commonly used intranuclear cascade FSI, this treatment changes the predicted inclusive cross sections [32]. Each calculation is made for an oxygen target, while the HF-CRPA model is also considered for carbon. Together, the considered models, summarized in Table I, cover a wide range of approaches to account for nuclear effects and represent those most commonly used for neutrino oscillation analyses. They further include model variations with key processes disabled which, while not realistic, provide a means to study their role.

TABLE I. The list of CCQE cross-section models used in this work. All are calculated for an oxygen target, other than HF-CRPA C.

Model	Description
SuSAv2	Model from [26]
HF	Model from [27] w/o CRPA corrections
HF-CRPA	w/ CRPA corrections
HF-CRPA PW[a]	w/ CRPA corrections, plane-wave nucleon
HF-CRPA C	w/ CRPA corrections, carbon target
SF	Model from NEUT based on [23]
SF w/o PB[a]	w/o Pauli blocking
SF M_A^{QE} 1.03	w/ modified nucleon axial mass
LFG	Model from NEUT based on [21]

[a]Models are not realistic but provide a study of disabling certain effects.

SuSAv2, HF-CRPA, SF, and LFG have been extensively compared with lepton scattering data, for example in Refs. [26,28–30,33–41]. SuSAv2, HF-CRPA, and SF have been shown to provide comparably good agreement with inclusive electron-scattering data. Overall, no model is able to provide a good description of global neutrino-scattering measurements, although the RPA suppression of the cross section at small energy transfers in the HF-CRPA and LFG models appears favored (although this is somewhat degenerate with the modeling of nonquasielastic processes).

A ratio between $\overset{(-)}{\nu}_e$ and $\overset{(-)}{\nu}_\mu$ differential cross sections across a range of incoming neutrino energy (E_ν) and outgoing lepton angles with respect to the incoming neutrino (θ) is defined as

$$R^{\text{Model}}_{\nu_\alpha/\nu_\beta}(E_\nu,\theta) = \left[\frac{d\sigma_{\nu_\alpha}}{d\cos\theta}\Big/\frac{d\sigma_{\nu_\beta}}{d\cos\theta}\right]^{\text{Model}}(E_\nu,\theta),$$

where α and β give the flavors under consideration. $R^{\text{SF}}_{\nu_e/\nu_\mu}$, $R^{\text{HF-CRPA}}_{\nu_e/\nu_\mu}$, $R^{\text{SF}}_{\bar{\nu}_e/\bar{\nu}_\mu}$, and $R^{\text{HF-CRPA}}_{\bar{\nu}_e/\bar{\nu}_\mu}$ are shown in Fig. 1 [25]. Note that the contour lines shown are built using a bilinear interpolation based on the four nearest bin centers [42] and that this uses unseen bins for $E_\nu < 0.2$ GeV. Large differences between the HF-CRPA and SF models are seen in the forward-scattered region, as previously studied in [15]. Although this behavior is also observed in SF, it is much weaker.

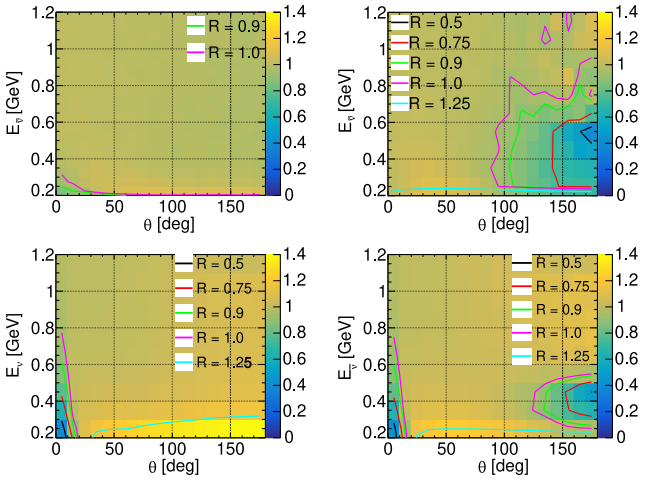

FIG. 1. $R^{\text{SF}}_{\nu_e/\nu_\mu}$ (top left), $R^{\text{HF-CRPA}}_{\nu_e/\nu_\mu}$ (bottom left), $R^{\text{SF}}_{\bar{\nu}_e/\bar{\nu}_\mu}$ (top right), and $R^{\text{HF-CRPA}}_{\bar{\nu}_e/\bar{\nu}_\mu}$ (bottom right) are shown as a function of outgoing lepton angle and the neutrino energy. The contour lines highlight the regions where the ratio significantly deviates from unity.

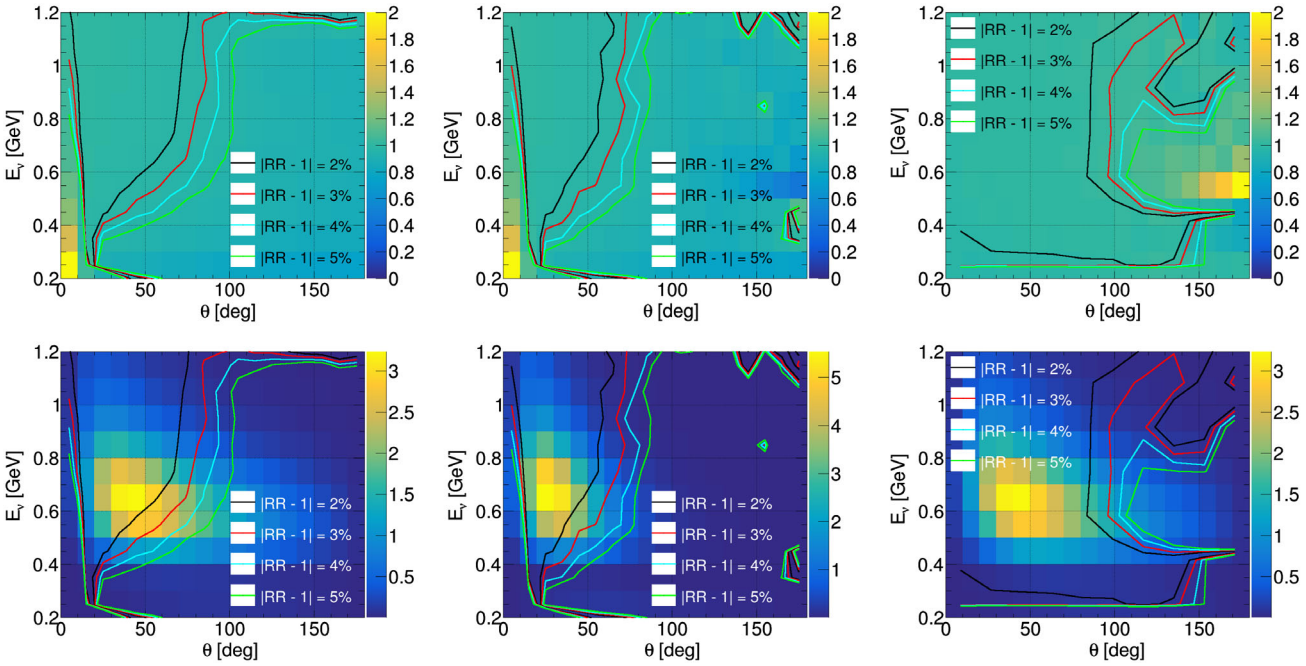

FIG. 2. The upper plots show $RR^{\text{HF-CRPA/SF}}_{\nu_e/\nu_\mu}$ (left), $RR^{\text{HF-CRPA/SF}}_{\bar{\nu}_e/\bar{\nu}_\mu}$ (center), and $RR^{\text{HF-CRPA/SF}}_{\nu_e/\bar{\nu}_e}$ (right) as a function of the outgoing lepton angle and neutrino energy. Contour lines highlight regions where $|RR_{\nu_e/\nu_\mu} - 1|$ differs from zero. The lower plots show the same contour lines overlaid on the oscillated event rates expected at the T2K/Hyper-K FD built using the SF model (the ν_e event rate is shown for the RR_{ν_e/ν_μ} and $RR_{\nu_e/\bar{\nu}_e}$ contours and the $\bar{\nu}_e$ rate is shown for the $RR_{\bar{\nu}_e/\bar{\nu}_\mu}$ contours) [25]. The z axes of the lower plots show the relative proportion of the event rate in each bin as a percentage.

To better quantify these deviations, the double ratio of the differential cross section predicted by two different models is computed as

$$RR^{\text{Model 1/Model 2}}_{\nu_\alpha/\nu_\beta}(E_\nu,\theta) = \frac{R^{\text{Model 1}}_{\nu_\alpha/\nu_\beta}(E_\nu,\theta)}{R^{\text{Model 2}}_{\nu_\alpha/\nu_\beta}(E_\nu,\theta)}.$$

$RR^{\text{HF-CRPA/SF}}_{\nu_e/\nu_\mu}$, $RR^{\text{HF-CRPA/SF}}_{\bar{\nu}_e/\bar{\nu}_\mu}$, and $RR^{\text{HF-CRPA/SF}}_{\nu_e/\bar{\nu}_e}$, are shown in Fig. 2. The forward-scattered region at angles below 20° show a large discrepancy between the models. However, it is interesting to see that the differences remain non-negligible when considering angles larger than about 50°

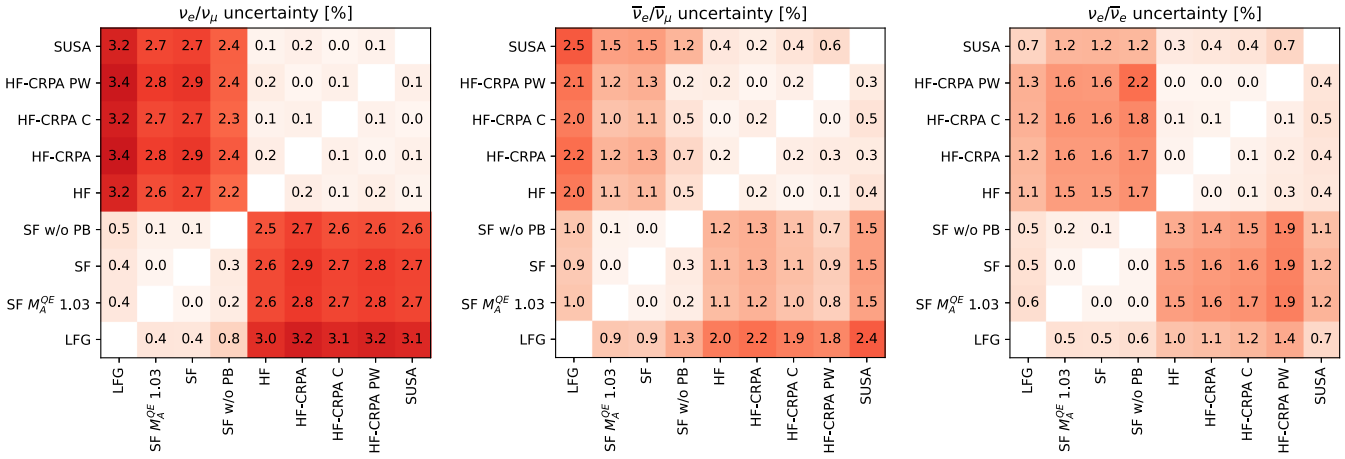

FIG. 3. The flux-averaged uncertainties in percent obtained by comparing the different cross-section models shown in Table I: Δ_{ν_e/ν_μ} (left), $\Delta_{\bar{\nu}_e/\bar{\nu}_\mu}$ (center), $\Delta_{\nu_e/\bar{\nu}_e}$ (right). The lower triangle is averaged over the event-rate distribution predicted by the model given on the horizontal axis, while the upper triangle contains the resulting values from the averaging over the model on the vertical axis, resulting in an asymmetric matrix.

for energies close to Hyper-K's oscillation maximum (~0.6 GeV).

In order to investigate the impact of potential cross-section mismodeling, the contours highlighting the regions with large $RR^{\text{HF-CRPA/SF}}_{\overset{(-)}{\nu}_e/\overset{(-)}{\nu}_\mu}$ are also shown overlaid on expected oscillated ν_e and $\bar{\nu}_e$ appearance event distributions at T2K/Hyper-K[1] in Fig. 2 [25].

From Fig. 2 it is clear that neither the large differences in the very forward region nor the differences at low neutrino energies will have any significant impact on T2K or Hyper-K oscillation analyses, as only a very small portion of CCQE interactions will fall within this region. However, it can also be seen that a sizable fraction of the interactions fall in the higher-angle region of the phase space where $RR^{\text{HF-CRPA/SF}}_{\overset{(-)}{\nu}_e/\overset{(-)}{\nu}_\mu}$ differs from unity by more than 2%. In the case of antineutrino interactions, which have a larger portion of their cross section at more forward outgoing lepton angles, the overlap with regions of large deviations from unity is smaller. The computed $RR^{\text{HF-CRPA/SF}}_{\nu_e/\bar{\nu}_e}$ is also shown, from which it can be seen that the regions with the largest deviations from unity overlap only with the extreme tails of the expected event distribution (i.e., at very low cross section).

An estimate of the integrated uncertainty on the expected $\overset{(-)}{\nu}_e$ appearance event rates associated with differences between $\overset{(-)}{\nu}_e$ and $\overset{(-)}{\nu}_\mu$ cross sections due the modeling of nuclear effects is computed by averaging the model differences over the distribution of events predicted with the SF model, as illustrated in the lower plots of in Fig. 2. The resultant uncertainties on the ν_μ/ν_e, $\bar{\nu}_\mu/\bar{\nu}_e$, and $\nu_e/\bar{\nu}_e$ cross-section ratios are defined, respectively, as $\Delta^{\text{Model 1/Model 2}}_{\nu_e/\nu_\mu}$, $\Delta^{\text{Model 1/Model 2}}_{\bar{\nu}_e/\bar{\nu}_\mu}$, and $\Delta^{\text{Model 1/Model 2}}_{\nu_e/\bar{\nu}_e}$. The former two are either fully correlated or fully anticorrelated, depending on whether the averaged model differences cause the cross-section ratios to change in the same direction.

The flux-averaged uncertainties derived for comparisons of each pair of models introduced in Table I are shown as a matrix in Fig. 3. This pairwise comparison derived from different model combinations permits an analysis of the possible physical source of differences in predictions of R_{ν_e/ν_μ}, $R_{\bar{\nu}_e/\bar{\nu}_\mu}$, and $R_{\bar{\nu}_e/\nu_e}$. Overall, every systematic alteration within a model is found to change the ratios of interest by less than 0.5%, while differences between models using different nuclear ground states (LFG, SuSAv2, SF-based, HF-based) are much larger (2–3%). This may suggest that the differences are driven by the treatment of the nuclear ground state. Note also that the change in the ratios for HF-CRPA between oxygen and carbon targets is much smaller than the differences between models, implying carbon-to-oxygen differences are likely to be a subdominant effect [25].

An indication of the impact of the derived uncertainties on neutrino oscillation analyses can be visualized using "bievent" plots. These show the expected $\nu_\mu \to \nu_e$ versus $\bar{\nu}_\mu \to \bar{\nu}_e$ appearance event rate at the FD for different values of the oscillation parameters. Such plots are shown for different values of δ_{CP}, the MO, and $\sin^2\theta_{23}$ in Fig. 4. The separation between different oscillation models is compared with the statistical uncertainty and the systematic uncertainty

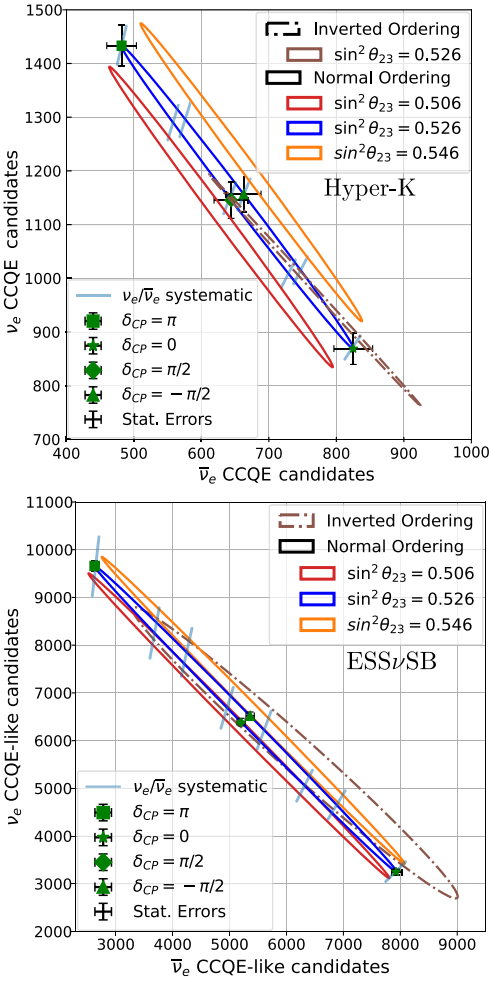

FIG. 4. Bievent plots for Hyper-K and ESSνSB, considering exposures of 2.7×10^{22} and 21.6×10^{22} protons on target, respectively (corresponding to 10 and 1 operational years) [6,8,25]. Each ellipse spans values of δ_{CP} while the different ellipses show variations to the MO and $\sin^2\theta_{23}$. For several points around one ellipse, the black bars show the expected experimental statistical uncertainty and the diagonal light-blue bar shows the modeling uncertainty from $\Delta^{\text{HF-CRPA/SF}}_{\nu_e/\bar{\nu}_e}$.

[1]The event rates are calculated using only CCQE interactions (using the SF model), without applying efficiency corrections or detector smearing. The oscillation parameters used are $\sin^2\theta_{12} = 0.297$, $\sin^2\theta_{13} = 0.0214$, $\sin^2\theta_{23} = 0.526$, $\Delta m^2_{21} = 7.37 \times 10^{-5}$, $|\Delta m^2_{32}| = 2.463 \times 10^{-3}$, $\Delta m^2_{32} > 0$ (normal ordering), $\delta_{CP} = 0$.

from $\Delta^{\text{HF-CRPA/SF}}_{\nu_e/\bar{\nu}_e}$ (while $\Delta^{\text{HF-CRPA PW/SF w/o PB}}_{\nu_e/\bar{\nu}_e}$ shows a larger uncertainty, it is a comparison of two unrealistic models). The uncertainties are shown to be comparable in size, but the latter is fully correlated between ν_e and $\bar{\nu}_e$. The propagation of the uncertainty through an oscillation analysis therefore mostly affects the sensitivity to the CP-conserving term (proportional to $\cos\delta_{CP}$) of the oscillation probability, rather than the CP-violating one (proportional to $\sin\delta_{CP}$). It does not extend the range of δ_{CP} values for which there is degeneracy between the different MO and δ_{CP} but it does enhance the existing significant degeneracy in regions where the ellipses for the different MO overlap. Figure 4 also shows that a stronger degeneracy is introduced in the measurement of $\sin^2\theta_{23}$, whose effect is correlated between ν_e and $\bar{\nu}_e$ events. The derived systematic uncertainty can therefore affect the determination of the θ_{23} octant.

Similar conclusions can be derived for an ESSνSB experimental configuration [25]. The largest deviation of $RR_{\nu_e/\bar{\nu}_e}$ from unity was found from the comparison of the SF and the HF-CRPA models, resulting in $\Delta_{\nu_e/\nu_\mu} = 6.4\%$, $\Delta_{\bar{\nu}_e/\bar{\nu}_\mu} = 2.2\%$, and $\Delta_{\nu_e/\bar{\nu}_e} = 4.2\%$, considerably larger than the uncertainties derived from the Hyper-K simulation. Bievent plots for ESSνSB are also shown in Fig. 4. The impact of the estimated systematic uncertainty is shown to be much larger than the projected statistical uncertainties and significantly impacts the sensitivity to determining the $\sin^2\theta_{23}$ octant. However, note that ESSνSB gains more from measurements of the shape of the oscillated spectrum which is not reflected in the bievent plots.

In conclusion, an evaluation of uncertainties on the $\overset{(-)}{\nu}_e/\overset{(-)}{\nu}_\mu$ and $\nu_e/\bar{\nu}_e$ cross-section ratios from the modeling of nuclear effects has been studied using the spread of predictions from a wide variety of models. Overall, it has been found that such uncertainties are unlikely to be dominant in measurements of $\sin\delta_{CP}$ term and the MO, although they may become crucial for analyses of $\cos\delta_{CP}$ and the $\sin^2\theta_{23}$ octant. More detailed studies are required in order to evaluate the impact of a systematic uncertainty affecting the modeling of the cross section as a function of FD observables. While this analysis has focused on CCQE interactions, analogous model discrepancies may exist for other processes and nuclei.

The authors would like to thank the T2K and Hyper-K collaborations, in particular for useful discussions in T2K's "Physics and Performance" and "Neutrino Interactions" working groups. The authors would like to thank Jan Sobczyk, Marco Martini, Claudio Giganti, and Anna Ershova for their insightful comments on a draft version of the manuscript. S. D. would like to especially thank Kevin McFarland, Laura Munteanu, and Callum Wilkinson for fruitful discussions. D. S. and T. Di. were supported by the Swiss National Science Foundation Eccellenza grant (Grant No. SNSF PCEFP2_203261), Switzerland. T. De. was supported by the Science and Technology Facilities Council (Grants No. ST/X002489/1 and No. ST/V006215/1). L. P. is supported by a Royal Society University Research Fellowship (Grant No. URF\R1\211661). Fermilab is operated by the Fermi Research Alliance, LLC under Contract No. DE-AC02-07CH11359 with the United States Department of Energy. S. B. was supported by CEA (France), Grant No. P2IO LabEx (ANR-10-LABX-0038) in the framework "Investissements d'Avenir" (ANR-11-IDEX-0003-01) managed by the "Agence Nationale de la Recherche" (ANR), France; H2020 Grant No. RISE-GA822070-JENNIFER2 2020.

[1] T2K Collaboration, Nature (London) **580**, 339 (2020); **583**, E16 (2020).
[2] K. Abe *et al.* (T2K Collaboration), Phys. Rev. D **103**, 112008 (2021).
[3] M. A. Acero *et al.* (NOvA Collaboration), Phys. Rev. Lett. **123**, 151803 (2019).
[4] M. A. Acero *et al.* (NOvA Collaboration), Phys. Rev. D **106**, 032004 (2022).
[5] K. Abe *et al.* (T2K, J-PARC Neutrino Facility Group), arXiv:1908.05141.
[6] K. Abe *et al.* (Hyper-Kamiokande Collaboration), arXiv:1805.04163.
[7] R. Acciarri *et al.* (DUNE Collaboration), arXiv:1512.06148.
[8] A. Alekou *et al.*, Eur. Phys. J. Spec. Top. **231**, 3779 (2022).
[9] L. Alvarez-Ruso *et al.*, Prog. Part. Nucl. Phys. **100**, 1 (2018).
[10] M. Scott, Proc. Sci. ICHEP2020 (2021), 174.
[11] A. Abed Abud *et al.* (DUNE Collaboration), Instruments **5**, 31 (2021).
[12] M. Martini, N. Jachowicz, M. Ericson, V. Pandey, T. Van Cuyck, and N. Van Dessel, Phys. Rev. C **94**, 015501 (2016).
[13] A. M. Ankowski, Phys. Rev. C **96**, 035501 (2017).
[14] A. Nikolakopoulos, V. Pandey, J. Spitz, and N. Jachowicz, Phys. Rev. C **103**, 064603 (2021).
[15] A. Nikolakopoulos, N. Jachowicz, N. Van Dessel, K. Niewczas, R. González-Jiménez, J. M. Udías, and V. Pandey, Phys. Rev. Lett. **123**, 052501 (2019).

[16] M. Day and K. S. McFarland, Phys. Rev. D **86**, 053003 (2012).
[17] K. Abe *et al.* (T2K Collaboration), Phys. Rev. Lett. **124**, 161802 (2020).
[18] O. Tomalak, Q. Chen, R. J. Hill, and K. S. McFarland, Nat. Commun. **13**, 5286 (2022).
[19] O. Tomalak, Q. Chen, R. J. Hill, K. S. McFarland, and C. Wret, Phys. Rev. D **106**, 093006 (2022).
[20] Y. Hayato and L. Pickering, Eur. Phys. J. Spec. Top. **230**, 4469 (2021).
[21] J. Nieves, I. Ruiz Simo, and M. J. Vicente Vacas, Phys. Rev. C **83**, 045501 (2011).
[22] B. Bourguille, J. Nieves, and F. Sánchez, J. High Energy Phys. 04 (2021) 004.
[23] O. Benhar, A. Fabrocini, S. Fantoni, and I. Sick, Nucl. Phys. **A579**, 493 (1994).
[24] P. Stowell *et al.*, J. Instrum. **12**, P01016 (2017).
[25] See Supplemental Material at http://link.aps.org/supplemental/10.1103/PhysRevD.108.L031301 for (i) a detailed analysis of statistical uncertainties associated with the NEUT event generation; (ii) details concerning the simulation of the T2K/Hyper-K and ESSνSB experimental configurations; (iii) further details regarding the change in the cross-section ratios of interest under the synthetic model tweaks, including the consideration of HF-CRPA differences on a carbon and oxygen target; and (iv) a data file containing the histograms used in the analysis.
[26] R. Gonzaléz-Jiménez, G. D. Megias, M. B. Barbaro, J. A. Caballero, and T. W. Donnelly, Phys. Rev. C **90**, 035501 (2014).
[27] N. Jachowicz, K. Heyde, J. Ryckebusch, and S. Rombouts, Phys. Rev. C **65**, 025501 (2002).
[28] V. Pandey, N. Jachowicz, T. Van Cuyck, J. Ryckebusch, and M. Martini, Phys. Rev. C **92**, 024606 (2015).
[29] S. Dolan, A. Nikolakopoulos, O. Page, S. Gardiner, N. Jachowicz, and V. Pandey, Phys. Rev. D **106**, 073001 (2022).
[30] S. Dolan, G. D. Megias, and S. Bolognesi, Phys. Rev. D **101**, 033003 (2020).
[31] C. Andreopoulos *et al.*, Nucl. Instrum. Methods Phys. Res., Sect. A **614**, 87 (2010).
[32] A. Nikolakopoulos, R. González-Jiménez, N. Jachowicz, K. Niewczas, F. Sánchez, and J. M. Udías, Phys. Rev. C **105**, 054603 (2022).
[33] M. B. Avanzini *et al.*, Phys. Rev. D **105**, 092004 (2022).
[34] G. D. Megias, J. E. Amaro, M. B. Barbaro, J. A. Caballero, and T. W. Donnelly, Phys. Rev. D **94**, 013012 (2016).
[35] G. D. Megias, J. E. Amaro, M. B. Barbaro, J. A. Caballero, T. W. Donnelly, and I. Ruiz Simo, Phys. Rev. D **94**, 093004 (2016).
[36] N. Jachowicz and A. Nikolakopoulos, Eur. Phys. J. Spec. Top. **230**, 4339 (2021).
[37] A. M. Ankowski, O. Benhar, and M. Sakuda, Phys. Rev. D **91**, 033005 (2015).
[38] K. Abe *et al.* (T2K Collaboration), Phys. Rev. D **101**, 112004 (2020).
[39] A. Papadopoulou *et al.* (Electrons for Neutrinos Collaboration), Phys. Rev. D **103**, 113003 (2021).
[40] M. Khachatryan *et al.* (CLAS, e4v Collaborations), Nature (London) **599**, 565 (2021).
[41] K. Abe *et al.* (T2K Collaboration), Phys. Rev. D **101**, 112001 (2020).
[42] F. Rademakers, R. Brun, P. Canal *et al.*, ROOT—An object-oriented data analysis framework. ROOT-project/ROOT: v6.10/04 (2017).